

Predicting Mammographic Breast Density Assessment Using Artificial Neural Networks

Soumaya Boujemaa¹, Youssef Bouzekraoui^{2*}, Farida Bentayeb²

1. Department of Physics, LPHE, Modeling and Simulations, Faculty of Science, Mohammed V University, Rabat, Morocco
2. Hassan First University of Settat, High Institute of Health Sciences, Laboratory of Sciences and Health Technologies, Settat, Morocco

| ARTICLE INFO | ABSTRACT |
|--|--|
| Article type: Original Paper | Introduction: Mammographic density is a significant risk factor for breast cancer. Classification of mammographic density based on Breast Imaging Reporting and Data System (BI-RADS) is usually used to describe breast density categories but the visual assessment can have some restrictions in a routine check in the screening mammography centers. The object of this study was to investigate the effectiveness of artificial neural networks in predicting breast density, based on the clinical patient dataset in a University hospital. |
| Article history: Received: Oct 22, 2022 Accepted: Feb 20, 2023 | Material and Methods: In this study, mammographic breast density was assessed for 219 women who underwent digital mammography screening using Volpara software. A model based on the Multi-Layer Perceptron Neural Network was trained to predict patient density by identifying the (dense vs. non-dense) breast density categories. The predictive model applied to the classification was examined by the Receiver operating characteristic (ROC) curve. |
| Keywords: Artificial Neural Networks Mammography Breast Density Breast Cancer | Results: The results show that the model predicted the breast density of patients with a classification rate of 98.2%. In addition, the area under the curve (AUC) was 0.998, signifying a high level of classification accuracy. Conclusion: The use of artificial neural networks is useful for predicting patients breast density based on clinical mammograms. |

► Please cite this article as:

Boujemaa S, Bouzekraoui Y, Bentayeb F. Predicting Mammographic Breast Density Assessment Using Artificial Neural Networks. Iran J Med Phys 2024; 21: 8-15. 10.22038/IJMP.2023.68587.2202.

Introduction

Cancer is the most common form of the disease in many countries and one of the leading causes of death. Breast cancer remains one of the most common cancers in women, and mammograms are a crucial part of prevention and detection. Mammography is an examination based on different levels of X-ray absorption for different breast tissues to detect breast diseases [1, 2, 3, 4, 5]. Despite the high sensitivity of mammography, higher density can reduce the efficacy of mammography screening [6, 7]. Studies have shown that higher density grades on mammograms increase the risk of developing breast cancer [8, 9, 10], and malignant tumors are less visible considering that they can be masked by dense tissue. Therefore, the classification of the breast density category is essential for detecting these lesions in dense mammograms.

Breast Imaging Reporting and Data System (BI-RADS) of the American College of Radiology reports the score of breast density, which assesses how much fatty, glandular, and fibrous tissue have in breasts [11, 12]. It categorizes breast density into four categories: Breasts with extremely dense fibroglandular tissue or heterogeneously dense breasts are categorized as

“dense,” while those with scattered fibroglandular tissue and largely fatty breasts are considered “non-dense” (Table1). Generally, radiologists can be confused with the two most common classified BI-RADS categories, “scattered fibroglandular tissue” and “heterogeneously dense breast” [13, 14].

Nowadays, the application of artificial intelligence in medical sciences has a great development worldwide, especially in cases of patient diagnosis [15]. Access to information about the patient's characteristics through the registration form, and the discharge summary contained within the health record for each patient provides actionable insights to improve diagnosis. By examining records and reports using the clinical imaging data system, radiologists can evaluate the breast density of patients, see what the category of BI-RADS is classified, and information into a final diagnosis by computerized tools.

Many data mining methods are utilized by researchers to analyze raw data and extract comprehensive information about patients and diagnostic strategies to enhance its functionality [16; 17]. Artificial neural networks (ANN) are an important aspect of intelligent learning methods. These

*Corresponding Author: Tel: +212623609312; Email: youssef0fsr@gmail.com

computational algorithms resemble the architecture of biological neurons and can solve complex problems. They are used for approximation and classification in various fields, especially in medical cases. A neural network is a data modeling tool that uses a nonlinear process, with inputs, outputs, and one or two hidden layers. The training algorithm adjusts the weights assigned to the connections between neurons in each layer to minimize errors and provide accurate predictions [18; 19].

The application of artificial intelligence in breast imaging is highly developed in various studies through in the identification, segmentation, and classification of lesions, breast density assessment, and breast cancer risk assessment [20; 21]. In this study, the ANN were developed to process a database corresponding to patients who underwent mammography examinations. Five variables were set as input variables, whereas results (dense vs. non-dense) were defined as classification variables.

The aim of this study was to examine whether an MLP neural network can help to predict patients' mammographic density resultants (dense vs. non-dense), by analyzing data obtained from automated Volpara software which estimates breast density based on the volume using the raw digital mammogram images.

Materials and Methods

Dataset

In the present work, patient data included information from 219 women's examinations where the raw data of the mammograms contain standard mammographic views (left and right breast in craniocaudal (CC) and mediolateral-oblique (MLO) view) performed using Siemens inspiration full-field digital mammography equipment in a Moroccan university hospital.

Breast density was estimated based on patient data using Volpara software (v1.5.2.1, Volpara Health Technologies, Wellington, New Zealand) on unprocessed DICOM images. The output of software tools are measurements of total breast volume, dense fibroglandular volume, breast tissue, percent volumetric breast density (VBD), the breast contact area between the breast and compression paddle, and glandularity for each image.

The Volpara Density software algorithm determines the attenuation of X-ray radiation between the image detector and the X-ray source based on the pixel signals of the mammography image. The pixel signal from pure adipose tissue is used as a reference and all other pixels are compared to this reference to calculate the thickness of adipose tissue and fibroglandular tissue. When calculating image size, the fat volume and

fibroglandular volume (FGV) in the entire breast are summed and their ratio is given as VBD (%).

The Volpara Density Grade (VDG) automated density scale is used to compare breast density and obtain the BI-RADS breast composition classification. The VDG is the threshold for VBD at various levels. VBD of less than 4.7% is in VDG 1, 4.7–7.9% is in VDG 2, 7.9%–15.5% is in VDG 3, and more than 15.5% is in VDG 4 [22; 23]. BI-RADS categories 1 and 2 are considered “non-dense” breasts and 3 and 4 are “dense” breasts corresponding to ACR BI-RADS (Table1).

Table1. Distribution of tissue density according to ACR BI-RADS category

| BI-RADS category | Density (%) | Breast density |
|------------------|-------------|--|
| I | 0-25 | Almost all fatty tissue (easiest to see anomalies or tumors) |
| II | 26-50 | Scattered areas of dense (fibrous and glandular) tissue, but mostly fatty tissue |
| III | 51-75 | Mix of dense and fatty tissue |
| IV | 76-100 | Mostly dense tissue (hardest to see tumors) |

The patient's ages ranged from 29 and 103 years, with a mean age of 51.8. The typical age group was 50-59 years (38.4 %) followed by 40-49 years (31.5%) (table2).

The proportion of dense breasts was 48.9%, while the non-dense breasts was 51.1% according to Volpara software using the BI-RADS categories. VDG 3 was the most common (33.8%) sample, followed by VDG 2 (29.7%). In the under 40 age group, VDG 4 was most common (39.1%) followed by VDG 3 (34.8%) (Table 1).

The VBD values computed by Volpara ranged from 3.7% to 30.3% (mean=9.2%). It was inversely related to age; Pearson correlation test reported a moderate correlation: $r=-0.404$ ($P<.001$).

The independent variables based on breast density measurements in this study were breast volume (BV), fibroglandular volume (FGV), compressed breast thickness (CBT), and contact area. The BV averaged 850.6 cm^3 , with a minimum volume of 141.4 cm^3 and a maximum volume of 2200.5 cm^3 . Thus, the FGV averaged 65.2 cm^3 , with a minimum volume of 20.5 cm^3 and a maximum volume of 214.4 cm^3 . Therefore, the contact area ranged from 4373.5 to 23661.1 mm^2 (mean= 10369 mm^2), and the CBT ranged from 23 to 80.5 mm (mean= 52.9). There was a strong linear correlation between BV and contact area: $r=0.823$ ($P<.001$), and between BV and CBT: $r=0.730$ ($P<.001$). However, a moderate correlation between VBD and contact area: $r=-0.527$ ($P<.001$).

Table 2. Distribution of Volumetric density grade (VDG) according to age groups

| Age | VDG 1 | | VDG 2 | | VDG 3 | | VDG 4 | | Total | |
|--------------------------------|-------|------|-------|------|-------|------|-------|------|-------|------|
| | N | (%) |
| <40 | 3 | 13.0 | 3 | 13.0 | 8 | 34.8 | 9 | 39.1 | 23 | 10.5 |
| 40-49 | 5 | 7.2 | 14 | 20.3 | 30 | 43.5 | 20 | 29.0 | 69 | 31.5 |
| 50-59 | 24 | 28.6 | 32 | 38.1 | 21 | 25.0 | 7 | 8.3 | 84 | 38.4 |
| 60-69 | 8 | 25.8 | 10 | 32.3 | 11 | 35.5 | 2 | 6.5 | 31 | 14.2 |
| >70 | 2 | 16.7 | 6 | 50.0 | 4 | 33.3 | 0 | 0.0 | 12 | 5.5 |
| Total (all patients& all ages) | 42 | 19.2 | 65 | 29.7 | 74 | 33.8 | 38 | 17.3 | 219 | 100 |

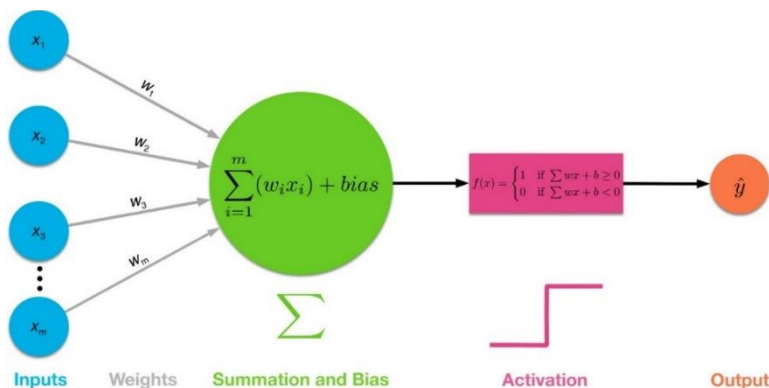


Figure 1. Multilayer Perceptron Neural Network architecture

ANN model

In this study, the prediction of breast density method was developed based on Multi-Layer Perceptron (MLP) Neural Networks trained with the back-propagation algorithm in IBM SPSS Statistics.

Supervised learning-based feed-forward neural networks are composed of an input layer, one or more hidden layers, and an output layer [24; 25]. The inputs are normalized between [0, 1] by the following equation:

$$X_{scaled} = \frac{x - \min(x)}{\max(x) - \min(x)}$$

Where x is the actual data, min(x) and max(x) are the minimum and maximum values in the input data respectively. Any layer created between the input layer and the output layer is referred to as the hidden layer. These layers are linked together through weights (Figure 1). The sigmoid activation function is used on the inputs to compute the output. The output of the neural network is given by the following equation: $Y = f(z) = \frac{1}{1+e^{-z}}$ and $z = \sum_{i=1}^n x_i w_i + b_i$

Where x_i are the inputs, w_i are the weights and b_i are the biases.

The network calculation consists of the training dataset, which is used to find the optimum weights using the back-propagation algorithm, then the testing data, which is used to find the errors and validate the previously trained model.

The datasets used to construct the ANN model were presented in Table 3. The data consisted of randomly

selected training subsets (74.4 %) and test subsets (25.6 %).

Table 3. Processing summary box

| | N | Percent |
|----------|----------|--------------|
| Sample | Training | 163 74.4% |
| | Testing | 56 25.6% |
| Valid | 219 | 100.0% |
| Excluded | 0 | |
| Total | 219 | |

The network diagram used by SPSS to predict density (dense, non-dense) based on independent variables is presented in Figure 2.

Five independent variables (Age, BV (cm³), FGV (cm³), compressed breast thickness (mm), and contact area (mm²)) were considered to build the ANN model. The automated structure selected five nodes in the hidden layer, while the output layer had two nodes to classify dense and non-dense categories. The activation function was the hyperbolic tangent for the hidden layer, whereas the output layer applied the softmax function. Cross-entropy was used as an error function for the softmax function.

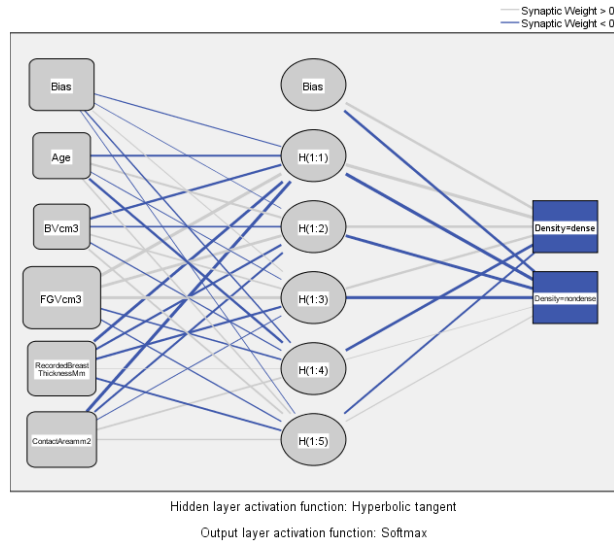


Figure 2. Artificial neural network diagram

Results

The results of the training and testing samples showed that the cross-entropy error for the training sample was 13.485, demonstrating the model's ability to predict breast density. The cross-entropy error was lower for the testing sample compared with the training dataset, meaning that the network model was not overfitted to the training data.

The percentage of incorrect predictions formed on training and testing samples was 3.1% and 1.8% respectively. Additionally, the instruction process was executed until one consecutive step without reducing the error function obtained in the testing sample.

The MLP network correctly classified 158 patients out of 163 in the training sample and 55 out of 56 in the testing sample. As a whole, 96.9% of training cases were properly classified. Table 4 presents the classification accuracy for the dependent variable breast density. In each case, the predicted density is indicated as dense if the predicted probability is above 0.5.

In the training sample, the sensitivity (true positive rate) given by equation 1 got 95.8%, while the specificity (or true negative rate) was 100% (equation 2). In addition, the precision (false positive) was 100% (equation 3), and the accuracy of the model (equation 4) was 98.2%. The MLP network model was classified as 0 patients as a false positive. This meant that the possibility of predicting a dense breast for a patient moving to a non-dense breast was minimal.

- True positive (TP) = $\frac{TP}{TP+FN} \times 100\%$ (1)
- True negative (TN) = $\frac{TN}{TN+FP} \times 100\%$ (2)
- False positive (FP) = $\frac{FP}{TP+FP} \times 100\%$ (3)
- False negative (FN) = $\frac{FN}{TN+FN} \times 100\%$ (4)

Different ANN structures with three layers and different number of neurons in the hidden layer were evaluated to select the best ANN model for predicting breast density. Input nodes and hidden nodes are shown in Table 5 to categorize dense and non-dense categories. The best model that predicted breast density for patients with a classification rate of 98.2% was constructed using five input nodes, 5 hidden nodes, and two output nodes.

For the dependent variable breast density, the graph presents box diagrams that categorize the predicted pseudo-probability dataset (Figure 3) [16]. For each box plot, values greater than 0.5 indicate correct predictions. From the left, the first box plot describes the predicted probability that the observed dense breast patients were in the dense breast category. The second box plot shows, the probability for a patient to be classified in the dense category, although it really was in the non-dense category. The third box plot shows patient density that has observed category non-dense, the predicted probability of category dense. The right box plot shows, the probability of a patient who has non-dense breasts being classified in the non-dense category.

Table 4. Accuracy of classification of training and testing sets

| Sample | Observed | Predicted | | Percent Correct |
|----------|-----------------|-----------|-----------|-----------------|
| | | dense | non-dense | |
| Training | dense | 77 | 3 | 96.3% |
| | non-dense | 2 | 81 | 97.6% |
| | Overall Percent | 48.5% | 51.5% | 96.9% |
| Testing | dense | 32 | 0 | 100.0% |
| | non-dense | 1 | 23 | 95.8% |
| | Overall Percent | 58.9% | 41.1% | 98.2% |

Table 5. Various structure characteristics of the ANN model

| Hidden layer | nodes | Accuracy (%) | AUC |
|--------------|-------|--------------|-------|
| 1 | 5 | 98.2 | 0.998 |
| 1 | 4 | 97 | 0.993 |
| 1 | 3 | 93.4 | 0.993 |
| 1 | 2 | 95.1 | 0.995 |
| 1 | 7 | 96.1 | 0.999 |
| 2 | 4-3 | 95.5 | 0.991 |
| 2 | 4-3 | 93.5 | 0.993 |

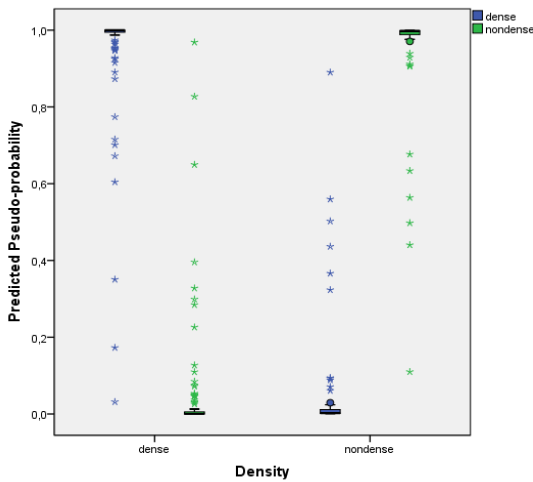


Figure 3. Predicted by observed graph

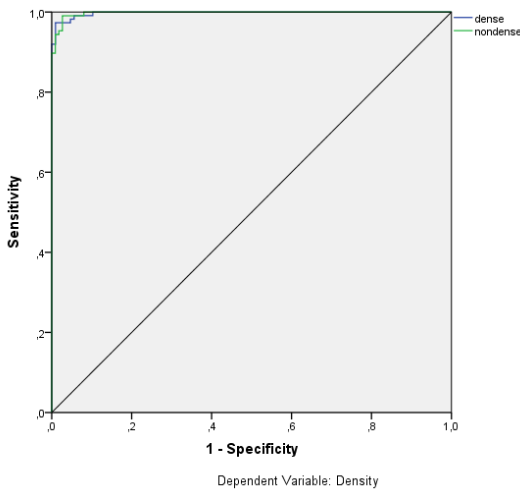


Figure 4. Receiver Operator Characteristic (ROC) curve

The model was evaluated according to the area under the ROC curve (AUC) to measure the predictive accuracy of the classification model. The ROC curve shows the relation between the true positive rate and false positive rate, based on the composite training and testing samples when varying the classification threshold (Figure 4). The model indicates a 0.998 probability that randomly selected patients from the dense category will have a higher model-predicted pseudo-probability of being in the dense category than randomly selected patients from the non-dense category.

All independent variables contribute to classifying dense and non-dense categories. Figure 5 presents the importance of independent variables in the ANN model. The effect of fibroglandular volume (cm^3) and the contact area (mm^2) were very powerful in the way the network classifies patients according to breast density. In addition, compressed breast thickness was also an important factor in the model compared with age and whole breast volume.

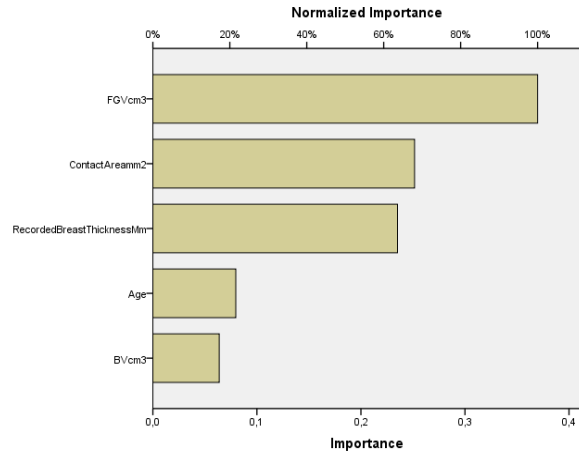


Figure 5. Independent variable importance graph

Discussion

Women with dense breasts can have a two- to six-fold increased risk of breast cancer compared to those with fatty breasts [26]. Therefore, it has been proposed that be informed to increase the frequency of screening and use a supplemental screening method such as ultrasound or magnetic resonance imaging in order to increase the probability of detecting breast cancer in the early stage. Adopting women who are most susceptible to benefit from additional or alternative screening methods requires the measures of breast density to report breast density grade. Therefore, several techniques based on mathematical models to compute breast density are expanded in order to improve objectivity in clinical assessments and to facilitate breast cancer research studies [27].

In this study, we evaluated the distribution of breast density in Moroccan women and the relevant related characteristics. Using Volpara software, volumetric breast density was assessed from digital mammograms. Qualitative visual evaluation based on BI-RADS is commonly used in clinical practice to report mammographic breast density. However, studies revealed that this visual evaluation showed varying degrees of agreement among radiologists [28; 29]. Radiologists may not often be able to reconstruct their evaluation due to confusion between “scattered density” and “heterogeneously dense”. Therefore, performing quantitative breast density measurements using automated computerized algorithms in screening centers is a requirement to provide an objective and reproducible assessment of breast density. To report to our country, screening mammography centers are

simply dependent on visual evaluation of breast density, and there are no automated measurements in clinical practice.

The percentage of dense breasts according to Volpara using the BI-RADS in our study was 51%. It was denser compared to Sartor et al, who found 43% (Sweden) and similar to Gemici et al and Brandt et al that showed 52,7% (Turkey) and 51%(USA) respectively, and lower dense compared to Tanaka et al indicated 85% (Japan) [30;31;32;33].

The grade of breast density was significantly moderate in the group of women who had aged 50-69 years; where VDG 4 (%) was 14.8%. We noted that the mean values of VBD were 7 % in this age range. Furthermore, women with large CBT were associated with lower density compared to small breast thickness; VDG 4 (%) was 10%, for CBT>60mm, whereas, for CBT<40mm, VDG 4 (%) reached 38%. The patients in the younger age group exhibited higher density for each CBT than those in the older group. The decrease in breast density with increased age is due to an increase for adipose tissue in the breast, as many authors have demonstrated, as well as those with higher CBT [34, 35].

In recent years, several scientists have focused their research on assessing and classifying breast density using diverse methodologies such as machine and deep learning techniques. The studies about feature-based methods included diverse approaches to show promising performance results as given by the study performed by Sharma et al. [36] where the mammograms were classified into two groups of Dense and Fatty using selected features and CFS + SMO Classifier and revealed an accuracy of 96.46%. Oliver et al. [37] used a set of 322 images to classify mammograms into two groups of Fatty and Dense using morphological and texture features and revealed an accuracy of 91%.

On the other hand, deep learning structures, as presented by Nan Wu et al. [38], investigated a deep learning-based approach using CNN to classify “dense” and “not dense” categories. In their report, 200000 images were used. The AUC was 0.832 when trained on 10% of the original training set. The accuracy of classification was 81.1%. Lehman et al [39] classified also mammograms into two groups, dense and non-dense, and reported an accuracy of 86.88%. They employed a deep CNN with 41479 images for training and 8677 for testing. In Lizzi et al [40] a residual neural network was applied to classify breast density according to two classes (fatty and dense) considering 7848 images. Classification accuracy for the two classes was 86.3%. In addition, Mohamed et al [41] applied a deep learning-based approach using CNN to distinguish BI-RADS density categories, “scattered density” versus “heterogeneously dense”. They reported an AUC of 92.6% and classification accuracy for the two classes was 98.8% from a cohort of 1427 patients with a large (22000 images) digital mammogram imaging dataset. In the study of Thomaz et al [42], mammograms were classified into four breast density classes according to

BI-RADS. An accuracy of 98.4% was reported by extracting features from the fully connected layer of the Convolutional Neural Network (CNN) and evaluating them using Multilayer Perceptron Neural Network (MLP-NN) classifier (Table 4). Seeing that the methods used in these studies and in our study are different, we cannot compare the results obtained, but we can have an idea about the efficiency of the proposed method.

Finally, the use of MLP neural network model to classify breast density (dense vs. non-dense) showed good classification performance. However, it is clear that the use of other functions is notable as well. Therefore, we suggest adopting deep learning models in our future work, such as convolutional neural network (CNN) algorithms, which are based on using original or pre-processed images as inputs for classification with an increase in the number of images.

Table 5. Performance of different types of classification models

| Studies references | Types of classification model | Accuracy (%) |
|-------------------------|-------------------------------|--------------|
| Sharma et al [35] | CFS + SMO | 96.46 |
| Oliver et al [36] | SFS + kNN | 91.00 |
| Wu, N. et al [37] | Baseline | 81.1 |
| | CNN | 86.5 |
| Lehman, C.D. et al [38] | ResNet-18 | 86.88 |
| Lizzi, F. et al [39] | CNN | 86.3 |
| Mohamed et al [40] | CNN | 98.8 |
| Thomaz et al [41] | MLP-NN | 98.4 |

Conclusion

In this paper, a multilayer perceptron neural network was trained by a back-propagation algorithm to predict patient breast density in routine mammograms. The classification performance in identifying the (dense vs. non-dense) breast density categories showed a promising accuracy rate of 98.2%. The findings of this study will be validated by analyzing a large clinical dataset in order to be used effectively as assistance to predict patient breast density in breast cancer screening.

References

1. Ghoncheh M, Pournamdar Z, Salehiniya H. Incidence and mortality and epidemiology of breast cancer in the world. *Asian Pacific journal of cancer prevention*. 2016 Jun 1;17(S3):43-6.
2. Narod SA. Reflections on screening mammography and the early detection of breast cancer. *Curr. Oncol*. 2014; 21: 210–4.
3. Sung H, Ferlay J, Siegel RL, Laversanne M, Soerjomataram I, Jemal A, et al. Global cancer statistics 2020: GLOBOCAN estimates of incidence and mortality worldwide for 36 cancers in 185 countries. *CA: a cancer journal for clinicians*. 2021 May;71(3):209-49.
4. Pwamang C, Sosu E, Schandorf C, Boadu M, Hewlett V. Assessment of dose to glandular tissue of patients undergoing mammography examinations. *J. Radiol. Radiat. Ther*. 2016;4:1062.
5. Pak F, Rashidy Kanan H. Improvement of breast cancer detection using non-sampled contourlet

- transform and super-resolution technique in mammographic images. *Iranian Journal of Medical Physics*. 2015 Mar 1;12(1):22-35.
6. Lyng E ,Vejborg I,Andersen Z ,von Euler-Chelpin M ,Napolitano G. Mammographic density and screening sensitivity, breast cancer incidence and associated risk factors in danish breast cancer screening. *J Clin Med*. 2019; 8.
 7. Nazari SS, Mukherjee P. An overview of mammographic density and its association with breast cancer. *Breast Cancer*. 2018; 25: 259–67.
 8. Duffy SW, Morrish OWE, Allgood PC, Black R, Gillan MGC, Willsher P, et al. Mammographic density and breast cancer risk in breast screening assessment cases and women with a family history of breast cancer. *Eur J Cancer*. 2018 Jan; 88:48-56.
 9. Eng A, Gallant Z, Shepherd J, McCormack V, Li J, Dowsett M, et al. Digital mammographic density and breast cancer risk: a case-control study of six alternative density assessment methods. *Breast Cancer Res*. 2014; 16:439–51
 10. Boyd NF, Martin LJ, Yaffe MJ, Minkin S. Mammographic density and breast cancer risk: current understanding and future prospects. *Breast Cancer Res*. 2011; 13:223–34.
 11. Boyd NF. Mammographic density and risk of breast cancer. *Am Soc Clin Oncol Educ Book*. 2013.
 12. Yaghjian L, Pinney S, Mahoney M, Morton A, Buckholz J. Mammographic breast density assessment: a methods study. *Atlas J Med Biol Sci*. 2011; 1:8–14.
 13. Huo CW, Chew GL, Britt KL. Mammographic density—a review on the current understanding of its association with breast cancer. *Breast cancer research and treatment*. 2014; 144(3):479–502.
 14. Eom HJ, Cha JH, Kang JW, Choi WJ, Kim HJ, Go E. Comparison of variability in breast density assessment by BI-RADS category according to the level of experience. *Acta Radiol*. 2018; 59: 527-32.
 15. Kanadpriya Basu, Ritwik Sinha, Aihui Ong, Treena Basu. Artificial Intelligence: How is It Changing Medical Sciences and Its Future? *Indian J Dermatol*. 2020 Sep-Oct; 65(5): 365–70.
 16. Youk JH, Gweon HM, Son EJ, Kim JA. Automated volumetric breast density measurements in the era of the BI-RADS Fifth Edition: a comparison with visual assessment. *AJR Am J Roentgenol*. 2016; 206: 1056-62.
 17. Oliver A, Tortajada M, Llado X, Freixenet J, Ganau S, Tortajada L, et al. Breast density analysis using an automatic density segmentation algorithm. *J Digit Imaging*. 2015; 28:604–12.
 18. Deo RC. Machine learning in medicine. *Circulation*. 2015 Nov 17;132(20):1920-30.
 19. Karabatak H. A new classifier for breast cancer detection based on Naïve Bayesian, *Meas. J. Int. Meas. Confed*. 2015; 72: 32-6.
 20. Bewal R, Ghosh A, Chaudhary A. Detection of Breast Cancer using Neural Networks-A Review. *J Clin Biomed Sci*. 2015 Dec;5(4):143-8.
 21. Pham BT, Nguyen MD, Bui KT, Prakash I, Chapi K, Bui DT. A novel artificial intelligence approach based on Multi-layer Perceptron Neural Network and Biogeography-based Optimization for predicting coefficient of consolidation of soil. *Catena*. 2019 Feb 1;173:302-11.
 22. D'Orsi CJ. Breast Imaging Reporting and Data System: breast imaging atlas: mammography, breast ultrasound, breast MR imaging. ACR, American College of Radiology; 2003.
 23. Highnam R, Sauber N, S Destounis JH, McDonald D. Breast Density into Clinical Practice. In *IWDM 2012: Proceedings of the 11th International Workshop on Breast Imaging*, Volume 7361 of Lect Notes Comput Sci. 2012; 466–73.
 24. Russell SJ, Norvig P. *Artificial Intelligence: A Modern Approach*. Prentice Hall, New Jersey, USA. 2016.
 25. Rokach L. Ensemble-based classifiers. *Artificial intelligence review*. 2010 Feb;33:1-39.
 26. Freer PE. Mammographic breast density: impact on breast cancer risk and implications for screening. *Radiographics*. 2015 Mar-Apr;35(2):302-15
 27. Sak MA, Littrup PJ, Duric N, Mullooly M, Sherman ME, Gierach GL. Current and future methods for measuring breast density: a brief comparative review. *Breast cancer management*. 2015 Sep;4(4):209-21.
 28. Lee HN, Sohn YM, Han KH. Comparison of mammographic density estimation by Volpara software with radiologists' visual assessment: analysis of clinical-radiologic factors affecting discrepancy between them. *Acta Radiol*. 2015; 56: 1061-8.
 29. Seo JM, Ko ES, Han BK, Ko EY, Shin JH, Hahn SY. Automated volumetric breast density estimation: a comparison with visual assessment. *Clin Radiol*. 2013; 68: 690-5
 30. Sartor H, Lång K, Rosso A, Borgquist S, Zackrisson S, Timberg P. Measuring mammographic density: comparing a fully automated volumetric assessment versus European radiologists' qualitative classification. *Eur Radiol*. 2016 Dec;26(12):4354-60.
 31. Brandt KR, Scott CG, Ma L, Mahmoudzadeh AP, Jensen MR, Whaley DH, et al. Comparison of clinical and automated breast density measurements: implications for risk prediction and supplemental screening. *Radiology*. 2016 Jun;279(3):710-9.
 32. Gemici AA , Arıbal E , Özyayın AN , Gürdal S Ö , Özçınar B , Cabioglu N , et al. Comparison of Qualitative and Volumetric Assessments of Breast Density and Analyses of Breast Compression Parameters and Breast Volume of Women in Bahcesehir Mammography Screening Project. *Eur J Breast Health*. 2020; 16: 110–6.
 33. Tanaka M, Irikoma M, Asanuma E, Kanzaki M, Muto S. Mammographic Breast Density: Comparison of Fully Automated Quantitative Assessment (VolparaTM) with Visual Qualitative Classification in a Japanese Population and Investigation of Factors Influencing Disagreement. *Ningen Dock International*. 2019; 6: 37-43.
 34. Checka CM, Chun JE, Schnabel FR, Lee J, Toth H. The relationship of mammographic density and age: implications for breast cancer screening. *AJR Am J Roentgenol*. 2012 Mar;198(3):W292-5. Doi: 10.2214/AJR.10.6049.

35. Sharma V, Singh S. CFS–SMO based classification of breast density using multiple texture models. *Medical & biological engineering & computing*. 2014 Jun;52:521-9.
36. Oliver A, Freixenet J, Marti R, Pont J, Pérez E, Denton ER, et al. A novel breast tissue density classification methodology. *Ieee transactions on information technology in biomedicine*. 2008 Jan 7;12(1):55-65.
37. Wu N, Geras KJ, Shen Y, Su J, Kim SG, Kim E, et al. Breast density classification with deep convolutional neural networks. In *Proceedings of the 2018 IEEE International Conference on Acoustics, Speech and Signal Processing (ICASSP)*, Calgary, AB, Canada, 15–20 April. 2018; 6682–6.
38. Lehman CD, Yala A, Schuster T, Dontchos B, Bahl M, Swanson K, et al. Mammographic breast density assessment using deep learning: clinical implementation. *Radiology*. 2019 Jan;290(1):52-8.
39. Lizzi F, Scapicchio C, Laruina F, Retico A, Fantacci ME. Convolutional neural networks for breast density classification: performance and explanation insights. *Applied Sciences*. 2021 Dec 24;12(1):148.
40. Mohamed AA, Berg WA, Peng H, Luo Y, Jankowitz RC, Wu S. A deep learning method for classifying mammographic breast density categories. *Medical physics*. 2018 Jan;45(1):314-21.
41. Thomaz RL, Carneiro PC, Patrocinio AC. Feature extraction using convolutional neural network for classifying breast density in mammographic images. In *Medical imaging 2017: Computer-aided diagnosis*. 2017; 10134:675-82.